Nuclear Instruments and Methods in Physics Research B 85 (1994) 849–855
North-Holland

NIM B
Beam Interactions with Materials & Atoms

PIXE analysis of cascade impactor samples collected at the Kruger National Park, South Africa

I. Salma [a,1], W. Maenhaut [a,*], J. Cafmeyer [a], H.J. Annegarn [b], M.O. Andreae [c]

[a] *Institute for Nuclear Sciences, University of Gent, Proeftuinstraat 86, B-9000 Gent, Belgium*
[b] *University of the Witwatersrand, Private Bag 3, P.O. Wits, 2050 Johannesburg, South Africa*
[c] *Max Planck Institute for Chemistry, P.O. Box 3060, D-55020 Mainz, Germany*

Aerosol samples were collected in parallel with eight-stage cascade impactors (CIs) and stacked filter units (SFUs) in the Kruger National Park, South Africa, in September–October 1992. The collections took place at a regional "background" site and near prescribed savanna fires. The results obtained by PIXE analysis from the 41 parallel daily samples at the regional site were compared in terms of concentration ratios CI/SFU for the coarse and fine size fractions. The overall average ratio (average over all samples and various elements) was 0.77 ± 0.07 (based on 17 elements) for the coarse size fraction and 0.65 ± 0.07 (based on 14 elements) for the fine particle fraction. Possible explanations for these lower than 1 ratios are presented. From the CI data average elemental mass size distributions and mass median aerodynamic diameters (MMADs) were calculated for the regional site and for the near-fire collections. It was found that the MMADs for S, Cl, K, Zn, and Br were much lower near the fires than in the regional samples. Multivariate source apportionment was applied to the regional CI data set, and this was done separately for the coarse and the fine particle fraction. Biomass burning appeared to be the major source for the elements K, Zn, Br, and Rb in the fine size fraction.

1. Introduction

Recent evidence and estimations suggest that biomass burning emissions and subsequent photochemical processes play an important role in atmospheric chemistry, climate and ecology over a large region of the Earth [1]. In order to investigate the environmental impact of tropical biomass burning, the Southern Tropical Atlantic Regional Experiment (STARE) was organized in 1992, and this included as a subprogram the Southern African Fire-Atmosphere Research Initiative (SAFARI-92). The field work for SAFARI-92 took place in southern Africa in August, September and October 1992, during the dry season. The goals of our contribution to SAFARI-92 were to study the amount and composition of aerosol particles produced by biomass burning, to characterize the chemical composition of aerosols on a regional scale, to identify the major sources of the regional atmospheric aerosol, and to evaluate the relative contribution from these sources, and in particular from biomass burning.

Our activity within SAFARI-92 involved aerosol collections at a number of ground-based sites (in South Africa, Namibia, and Zimbabwe) and with airplanes, and analysis of the samples by various analytical techniques. However, the present paper is essentially limited to the presentation and discussion of data that were obtained by particle-induced X-ray emission (PIXE) analysis of cascade impactor (CI) samples collected in the Kruger National Park, South Africa. The data from these CI samples are compared with those derived from PIXE analysis of stacked filter unit samples, collected in parallel, and the performance and quality of the sampling/PIXE analysis combination for the two sampler types are evaluated. Furthermore, the results of the detailed CI size distribution measurements and of a multivariate receptor modelling on the CI data set are briefly discussed.

2. Experimental

2.1. Sampling

All samples discussed in this paper were collected inside the Kruger National Park, either at a fixed, regional "background" site (Skukuza) or near prescribed savanna fires. Two different types of size-frac-

* Corresponding author, phone +32 9 264 6579, fax +32 9 264 6699.
[1] On leave from Research Institute for Atomic Energy, P.O. Box 49, H-1525 Budapest, Hungary.

SSDI 0168-583X(93)E0557-W

tionating collection devices were employed, i.e., single-orifice cascade impactors (CI) and stacked filter units (SFUs). The CI was a Battelle-type cascade impactor from PIXE International Corporation (P.O. Box 2744, Tallahassee, FL 32316, USA) [2,3]. This device operates at a nominal flow rate of 1 l/min, it has seven impaction stages (numbered 7 through 1), and a backup filter stage, and the cut-off diameters for 50% collection efficiency (d_{50}-values) of the 7 impaction stages are 16, 8, 4, 2, 1, 0.5, and 0.25 μm equivalent aerodynamic diameter (EAD). As impaction foils we used 1.5 μm thick KIMFOL polycarbonate film, which was coated with a thin layer of vaseline (for stages 7 through 2) or paraffin (stage 1). A 0.4 μm pore size Nuclepore polycarbonate filter served as backup filter. The SFU was a home-built instrument, but was based on principles and SFU variants described in the literature [4–6]. The "Gent" SFU operates at a flow rate of 15–16 l/min, and utilizes two 47 mm diameter Nuclepore polycarbonate filters, with pore sizes of 8 μm (Apiezon-coated) and of 0.4 μm, which are placed in series. Upstream of the coarse filter is a pre-impaction stage, which intercepts the particles larger than 10 μm EAD. At the flow rate of 15–16 l/min, the coarse Nuclepore filter has a d_{50}-value of 2 μm EAD, so that the coarse filter then collects the 2–10 μm EAD size fraction, whereas the fine filter collects the particles < 2 μm EAD.

One CI and one SFU sampler were installed side by side at Skukuza, and operated from 1 September to 12 October 1992. Both samplers had their air intake facing downward, at about 1.8 m above ground. The collection time per sample was 24 h, each collection started typically at 8 a.m. local time, and a total of 41 parallel samples were collected. In addition to these regional samples, 5 sample pairs were collected near prescribed savanna fires inside the Kruger park. The collection time for these fire samples varied from 20 to 60 min.

2.2. Analysis

All CI samples (impaction films and backup filters), quarter sections of the SFU filter samples, and a number of field blanks for each collection material were analyzed by PIXE at Gent, using a proton beam of 2.4 MeV. The experimental setup and analytical procedures have been described in detail previously [7–9]. The beam area and beam current at the target depended on the size of the aerosol deposit and were either 0.54 cm^2 and 150 nA (for CI stages 7, 6, backup filters, and SFU filter sections) or 0.18 cm^2 and 50 nA (for CI stages 5 through 1). The X-ray spectra were typically accumulated for a preset charge of 60–80 μC with the larger beam and for 30 μC with the smaller beam. The PIXE spectra were fitted for 26 elements

Table 1
Average CI/SFU concentration ratios and associated standard deviations, based on 41 sample pairs from Skukuza, and average fine-to-coarse ratios with standard deviations and median atmospheric concentrations in the coarse size fraction, as derived from the 41 Skukuza CI samples

Element	Average CI/SFU concentration ratio		Mean fine-to-coarse ratio (CI) [a]	Coarse fraction (CI) Median atm. conc. (ng/m^3) [a]
	Fine fraction	Coarse fraction [a]		
Na	0.55 ± 0.11	0.68 ± 0.15	0.42 ± 0.14	440
Mg	0.70 ± 0.13	0.86 ± 0.12	0.35 ± 0.08	107
Al	0.59 ± 0.12	0.80 ± 0.19	0.13 ± 0.07	250
Si	0.68 ± 0.18	0.75 ± 0.08	0.12 ± 0.03	710
S	0.69 ± 0.21	0.65 ± 0.08	4.3 ± 2.3	110
Cl	10.8 ± 10.4	0.83 ± 0.17	0.22 ± 0.12	890
K	0.62 ± 0.13	0.74 ± 0.09	0.97 ± 0.56	112
Ca	0.83 ± 0.12	0.77 ± 0.08	0.21 ± 0.05	115
Ti	0.57 ± 0.10	0.78 ± 0.10	0.11 ± 0.03	27
Mn	0.65 ± 0.11	0.78 ± 0.17	0.13 ± 0.04	5.8
Fe	0.59 ± 0.11	0.78 ± 0.09	0.11 ± 0.03	230
Ni	–	0.84 ± 0.13	0.41 ± 0.26	0.32
Cu	0.58 ± 0.12	0.75 ± 0.21	0.44 ± 0.46	0.68
Zn	0.71 ± 0.16	0.64 ± 0.11	1.23 ± 0.48	1.07
Br	0.88 ± 0.25	0.88 ± 0.21	2.5 ± 1.6	1.49
Sr	0.64 ± 0.16	0.80 ± 0.15	0.25 ± 0.09	1.82
Zr	–	0.69 ± 0.16	0.21 ± 0.12	0.87
Pb	0.65 ± 0.13	–	3.2 ± 1.4	0.54

[a] The data for the coarse size fraction of the CI are the sums from stages 4 and 5 (see text).

(i.e., Na, Mg, Al, Si, P, S, Cl, K, Ca, Ti, V, Cr, Mn, Fe, Ni, Cu, Zn, Ga, As, Se, Br, Rb, Sr, Y, Zr, and Pb) with the computer program AXIL-84 [9]. The net peak areas obtained were corrected iteratively for X-ray attenuation, elemental amounts were derived using calibration factors, and, finally, atmospheric concentrations (in ng/m^3) were calculated. The SFU filters were also analyzed by instrumental neutron activation analysis (INAA) for up to 39 elements with procedures similar to those described earlier [10], by a light reflectance technique for determining black carbon, and by gravimetry to measure the particulate mass. The agreement between the PIXE and INAA data of the SFU filters was typically better than 10% for those elements that were measured with good precision in the two techniques.

3. Results and discussion

3.1. Comparison of data from parallel samples

In order to be able to compare the data from the two different aerosol samplers, the results from the CI were summed over various impaction stages. Thus, the data from the backup filter and stages 1 through 3 of the CI were added up to obtain the CI size fraction of < 2 μm EAD, which corresponds to the fine aerosol fraction of the SFU. Since the d_{50}-value (of 10 μm EAD) for the pre-impaction stage of the SFUs did not correspond to any of the d_{50}-values of the CI, two different sets of coarse CI data were calculated for comparison with the SFU coarse filter data. For the first set, the sums from stages 4 and 5 were used, thus representing the size fraction 2–8 μm EAD, and the second set included the data from stages 4 through 6, thus corresponding to the 2–16 μm EAD size fraction. In comparing the CI and SFU data sets, PIXE data were used exclusively, and the comparisons were done in terms of concentration ratios CI/SFU. Such ratios were calculated per element and per size fraction for each sample pair from Skukuza, and subsequently averaged over all 41 Skukuza sample pairs. In calculating the averages and associated standard deviations, evident outlier ratios or ratios with a percentage analytical standard deviation of larger than 30–35% were excluded. However, the total number of rejected outliers remained limited to less than 3%. The average CI/SFU ratios are presented in Table 1. For the coarse size fraction, the ratios obtained on the basis of the sums from CI stages 4 and 5 (first coarse CI data set) are listed. The corresponding ratios, using the sums from CI stages 4 through 6, were typically about 30% higher. Also presented in Table 1 are the average fine-to-coarse elemental concentration ratios and the median atmospheric concentrations in the coarse size fraction, as derived from the 41 CI samples from Skukuza. For the coarse fraction in those data, again the sum of stages 4 and 5 was used.

From a close observation of the various average CI/SFU ratios in Table 1, several features become apparent. First, the associated standard deviations are typically of the order of 20%, thus indicating that the ratios did not exhibit large variability from sample to sample. Secondly, with the exception of the data for fine Cl, all CI/SFU ratios are clearly less than 1, and this is more so for the fine size fraction than for the coarse fraction. On the other hand, within each size fraction the ratios seem to vary quite little from element to element. For the coarse size fraction, the overall average ratio and associated standard deviation (average over all elements) are 0.77 ± 0.07 and the corresponding data for the fine size fraction (when leaving out Cl and Br from the averaging) are 0.65 ± 0.07. Several explanations could be invoked for the systematically lower than 1 ratios. These include (a) bias in the air volume measurements for the CI and/or for the SFU, (b) deviation of the actual d_{50}-values from the nominal ones (e.g., the separation between fine and coarse could be different for CI and SFU), (c) wall losses and/or bounce-off effects in the CI, and (d) errors in the PIXE analysis. The last explanation can be rejected, as both the CI and SFU samples were analyzed with the same PIXE setup, using the same calibration factors and similar irradiation conditions, and as there is no element-dependency in the CI/SFU ratios. Any bias in the PIXE analysis (e.g., in the calibration factors, dead time correction, beam charge integration) would have worked in the same direction for the two sample types, and thus have cancelled out in calculating the ratios. As to a possible error in the air volume measurement, the volume meters used in the field were calibrated versus various other devices, including a mass flow meter, and it was concluded from this that the air volumes should be accurate to within 5%. With regard to deviations in the d_{50}-values, the separation between fine and coarse could well be somewhat different for the CI and the SFU. However, if this would be a serious problem, one would expect that the CI/SFU ratios would be very dependent upon the size distribution of the element. The fact that elements such as S, K, Zn, and Pb, which have much larger fine-to-coarse ratios than most of the other elements, exhibit very similar CI/SFU ratios as those other elements indicates that the fine/coarse separation for the SFU is quite close to the d_{50}-value for stage 4 of the CI. For the coarse size fraction, the less than 1 ratios could be partly attributable to the difference in upper cut-off (i.e., 10 μm EAD for the coarse filter of the SFU, 8 μm EAD for the CI). However, even when the sums of stages 4 through 6 (thus up to 16 μm EAD) are used for the CI, the overall average

CI/SFU ratio (and associated standard deviation) only becomes 0.99 ± 0.11. It seems therefore that the major reason for the low CI/SFU ratios in Table 1 has to be sought in cascade impactor sampling artifacts, i.e., in wall losses and bounce-off effects. It should be indicated here that only the central area of each CI impaction film was analyzed by PIXE (see section 2.2). The PIXE beam definitely enveloped the visible aerosol deposit, but as a result of bounce-off effects during the sampling, some aerosol particles may have ended up on the impaction film outside of the area analyzed by PIXE. Apparently, the cascade impactor artifacts are more severe for the fine size fraction than for the coarse particles. Overall, however, the differences observed here are not larger than those observed in other studies with parallel cascade impactor and filter samplings (see ref. [11] for a recent example of such study).

One CI/SFU ratio that really stands out in Table 1 is that for Cl in the fine size fraction. Furthermore, this ratio varied very much from sample to sample (from 1 up to 40). Similar very large discrepancies between Cl filter and cascade impactor data were also observed in a study on continental aerosols near Beijing, China [12]. Most likely, the discrepancies have to be attributed to Cl loss from the fine Nuclepore filters during the sampling (and possibly also during filter storage prior to analysis). Possible causes for the Cl loss are reactions on the filter of the Cl-containing aerosol particles with acidic particles (e.g., H_2SO_4) or with reactive gaseous species (i.e., acids or oxidants), which may both lead to the formation of volatile compounds of Cl (e.g., HCl) [13,14]. Support for such explanation was provided by the fact that the SFU/CI ratio for fine Cl was inversely related to the concentration of fine S. The Cl-loss mechanisms just discussed could in principle also be operative within the CI, but this device has the advantage that the fine Cl-containing particles are collected in four different stages (i.e., stages 3, 2, 1, and the backup filter). Because of the difference in size distributions, most of the fine Cl was collected on stage 3, whereas only a small fraction of the fine S was collected on this same stage.

3.2. Average size distributions

Elemental mass size distributions provide valuable information on the source processes for the particulate trace elements and on the transformation processes during atmospheric transport. From the CI data average elemental mass size distributions were calculated for the regional site (Skukuza) and for the near-fire collections. And on the basis of these average size distributions, average mass median aerodynamic diameters (MMADs) were subsequently derived for the two

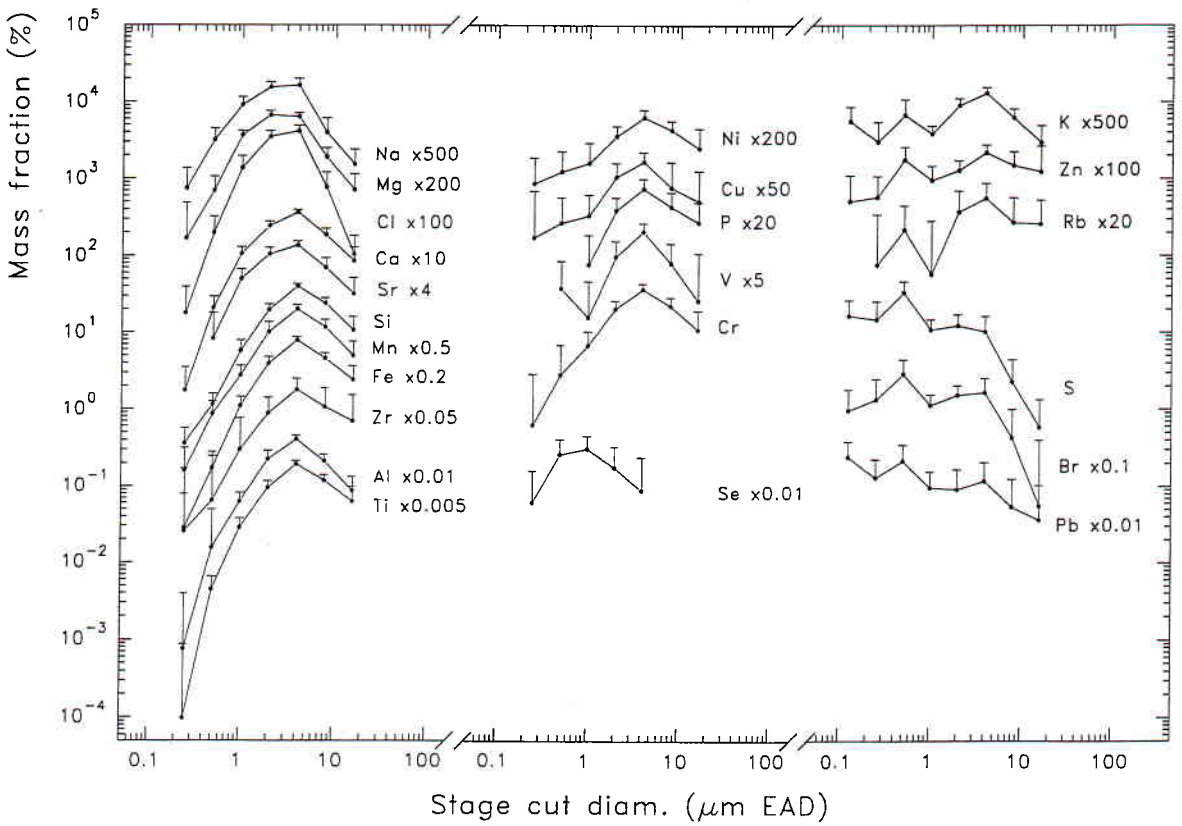

Fig. 1. Average mass size distributions for 23 elements at Skukuza. The data are mean mass fractions and standard deviations, based on 41 cascade impactor samples. For the filter stage, the d_{50}-value was set at 0.125 μm EAD.

Table 2
Average elemental mass median aerodynamic diameters (in μm EAD), as derived from the CI samples collected at Skukuza and near the prescribed savanna fires

Element	Skukuza	Fires
Na	3.5	1.89
Mg	3.6	5.6
Al	5.6	8.2
Si	6.1	10.1
P	6.4	6.4
S	0.75	0.42
Cl	4.0	0.38
K	3.2	0.31
Ca	5.1	6.9
Ti	6.3	9.5
V	5.2	–
Cr	5.8	–
Mn	6.0	6.7
Fe	6.1	9.1
Ni	5.5	11.7
Cu	5.0	7.2
Zn	3.8	0.35
Ga	5.3	–
Se	1.32	–
Br	0.96	0.23
Rb	5.0	–
Sr	4.8	6.7
Zr	6.3	–
Pb	0.74	–

types of samples. The MMADs are presented in Table 2, and the average size distributions for Skukuza are displayed in Fig. 1. For Skukuza, the various elements can be classified into three groups. A first group comprises Na, Mg, Al, Si, P, Cl, Ca, Ti, V, Cr, Mn, Fe, Ni, Cu, Sr and Zr. All these elements have essentially a unimodal size distribution, most of their mass occurs in supermicrometer particles (see also the average fine-to-coarse ratios in Table 1), and their MMADs are of the order of 4 to 6 μm EAD. Most likely, these elements are mainly attributable to dispersion processes, i.e., soil dust dispersal and/or sea spray. The elements in the second group (i.e., K, Zn, and Rb) also have a large MMAD (of 3–5 μm EAD), but, in contrast to those in the first group, they clearly have a bimodal size distribution. Also the third group of elements (with S, Br, and Pb) exhibits a bimodal size distribution, but most of their mass is in the fine size fraction (see also the last column of Table 1), and, as a consequence, their MMADs are below 1 μm EAD. The fine mode for the second and third group points to a high-temperature source for the elements in those groups. Most likely, this source is biomass burning and/or fossil fuel combustion.

The average elemental mass size distributions for the near-fire samples (not shown here) differed significantly from those for the regional samples. For the coarse mode, the maximum in the size distribution was generally shifted towards larger particle sizes, whereas, for the fine mode, it was shifted towards the finer particle sizes. As a result, noteworthy differences were also observed in the MMADs of the two types of samples (see Table 2). The MMADs for the typical soil dust elements (Al, Si, Ti, Fe) are all much larger near the fires than at the Skukuza site. Moreover, the atmospheric concentrations of these elements were also much enhanced near the fires. Both observations indicate that savanna fires are efficient mobilizers of soil dust into the atmosphere, as was recently also found by Gaudichet et al. [15]. For S, Cl, K, Zn, and Br in the near-fire samples, the average MMADs are of the order of 0.2–0.4 μm EAD, and, in addition, these elements had their maximum concentration on the filter stage (S, K, Zn, Br) or on stage 1 (Cl). This points to a nearby high-temperature source for these elements, which, undoubtedly, is the burning of the savanna.

3.3. Receptor modelling

In order to identify the major aerosol sources for the regional site, and to apportion the various elements to these sources, the Skukuza CI data set was subjected to an absolute principal component analysis (APCA) with VARIMAX rotation. The APCA procedure followed was identical to that described by Maenhaut and Cafmeyer [16], and it was applied separately to each of the two coarse fraction CI data sets (with the sums from stages 4 and 5, and from stages 4 through 6, respectively) and to the fine size fraction CI data set. For the coarse fraction, we will only present the results for the second data set, but those for the first data set were very similar.

For the coarse fraction, 20 elements were included in the APCA, i.e., Na, Mg, Al, Si, P, S, Cl, K, Ca, Ti, V, Mn, Fe, Ni, Zn, Ga, Br, Rb, Sr, and Zr. The variance in the data set was essentially explained by two components, and these were identified as soil dust and sea-salt. Most of the elements were fully attributed to one of the two components (with sea-salt being responsible for all the Na, Cl, S, and Br). Only four elements had significant contributions from the two sources, i.e., Mg, K, Ca, and Sr. Mg was apportioned for 25% to soil and for 75% to sea-salt. K and Ca, on the other hand, were attributed for 75% to soil and for 25% to sea-salt.

For the APCA on the fine size fraction, 16 elements were included, i.e., Na, Mg, Al, Si, S, Cl, K, Ca, Ti, Mn, Fe, Zn, Br, Rb, Sr, and Pb. Three components were retained, and they explained 87% of the variance in the data set. These components were identified as soil dust, sea-salt, and a biomass burning component.

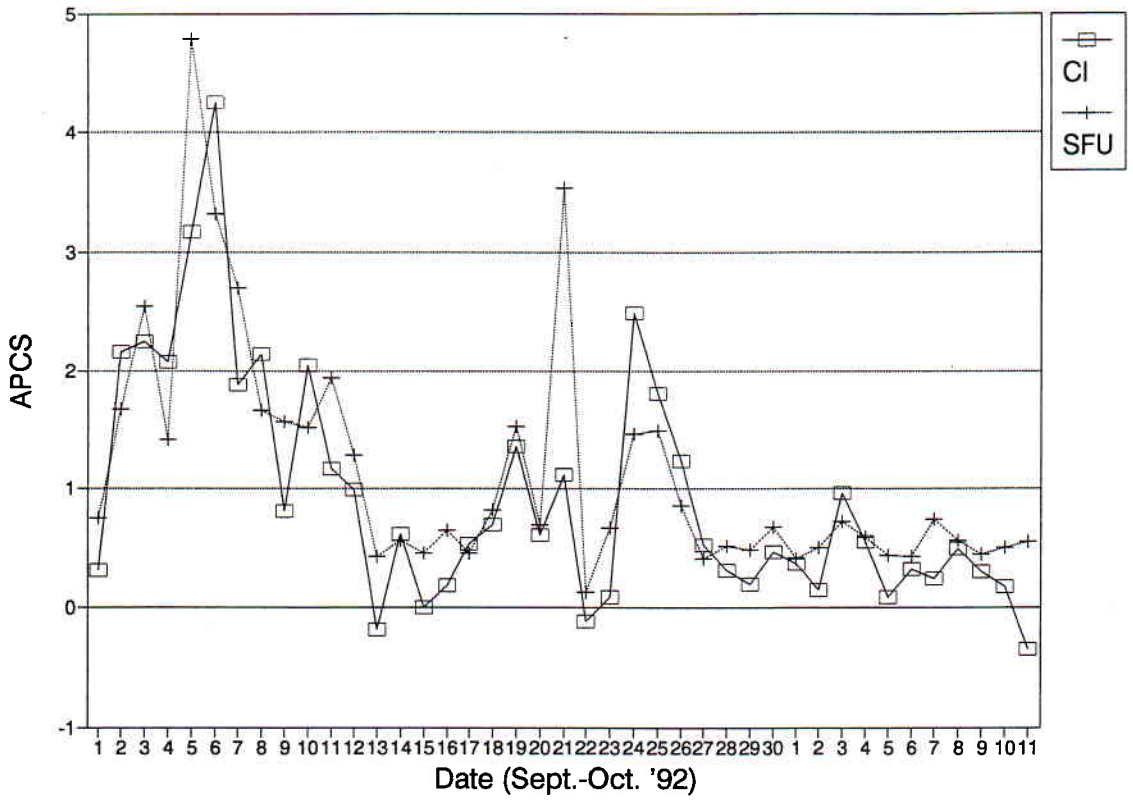

Fig. 2. Absolute principal component scores (APCS) for the biomass burning component at Skukuza, as obtained by APCA on (a) the data for the fine fraction of the cascade impactor samples and (b) the data for the fine filter of SFU samples collected in parallel (41 samples in each case).

Only four elements seemed to be really associated with the last component, i.e., K, Zn, Br and Rb, with loadings of 0.87, 0.48, 0.71 and 0.90, respectively. These elements were on the average for about 50% attributed to the biomass burning. However, the importance of the biomass burning component varied much from sample to sample. This is illustrated by the time trend of the absolute principal component scores (APCS) for this component, which is displayed in Fig. 2. The APCS for a component are a measure of the intensity (importance) of the component for each individual sample included in the APCA. For comparison, Fig. 2 also shows the APCS, as obtained from an APCA on the full data set of the fine SFU filter samples (thus including INAA elements, black carbon and particle mass). Although there are a few serious discrepancies between the two sets of APCS (particularly for the parallel samples collected on 21 September), overall, the agreement is quite satisfactory. Both APCS trends clearly show that the intensity of the biomass burning component was largest during the first two weeks of the sampling campaign.

Acknowledgements

This work is funded under contract no. GC/02/001 by the Impulse Programme "Global Change", which is supported by the Belgian State, Prime Minister's Service, Science Policy Office. Partial financial assistance is also provided by the Belgian "Nationaal Fonds voor Wetenschappelijk Onderzoek" and the "Interuniversitair Instituut voor Kernwetenschappen".

References

[1] P.J. Crutzen and M.O. Andreae, Science 250 (1990) 1669.
[2] R.I. Mitchell and J.M. Pilcher, Ind. Eng. Chem. 51 (1959) 1039.
[3] S. Bauman, P.D. Houmere and J.W. Nelson, Nucl. Instr. and Meth. 181 (1981) 499.
[4] T.A. Cahill, L.L. Asbaugh, J.B. Barone, R.A. Eldred, P.J. Feeney, R.G. Flocchini, C. Goodart, D.J. Shadoan and G.W. Wolfe, J. Air Pollut. Control Assoc. 27 (1977) 675.
[5] N.Z. Heidam, Atmos. Environ. 15 (1981) 891.
[6] W. John, S. Hering, G. Reischl, G. Sasaki and S. Goren, Atmos. Environ. 17 (1983) 373.
[7] W. Maenhaut, A. Selen, P. Van Espen, R. Van Grieken and J.W. Winchester, Nucl. Instr. and Meth. 181 (1981) 399.
[8] W. Maenhaut and H. Raemdonck, Nucl. Instr. and Meth. B 1 (1984) 123.
[9] W. Maenhaut and J. Vandenhaute, Bull. Soc. Chim. Belg. 95 (1986) 407.
[10] P. Schutyser, W. Maenhaut and R. Dams, Anal. Chim. Acta 100 (1978) 75.

[11] W. Maenhaut, G. Ducastel, R. Hillamo, T. Pakkanen and J.M. Pacyna, J. Radioanal. Nucl. Chem. 167 (1993) 271.
[12] J.W. Winchester, M.-X. Wang, L-X. Ren, W.-X. Lü, H.-C. Hansson, H. Lannefors, M. Darzi and A.C.D. Leslie, Nucl. Instr. and Meth. 181 (1981) 391.
[13] W. Maenhaut, H. Raemdonck and M.O. Andreae, Nucl. Instr. and Meth. B 22 (1987) 248.
[14] H. Raemdonck, W. Maenhaut and M.O. Andreae, J. Geophys. Res. 91 (1986) 8623.
[15] A. Gaudichet, F. Echalar, B. Chatenet, J.P. Quisefit, G. Malingre, H. Cachier, P. Buat-Ménard, P. Artaxo and W. Maenhaut, J. Atmos. Chem. (1993) in press.
[16] W. Maenhaut and J. Cafmeyer, J. Trace Microprobe Techn. 5 (1987) 135.